



Settlement Estimation Procedure: Box Excavations & Shafts 1D0101-G0G00-01004

Custodian

Mr [REDACTED]

CONFIDENTIALITY

This document contains proprietary information which shall not be reproduced without the permission of the CLRL Chief Executive

REVISION HISTORY						
Rev	Date	Prepared	Review	Approved	Accepted	Description
B	14/11/07	GA	DIH	DIH	MB	Typos in equations corrected
A	08/11/04	JNF	DIH	DIH	MB	First Issue

NOTE

Notify the Custodian of all errors, omissions and suggested improvements.

Cross London Rail Links Limited
1, Butler Place
LONDON
SW1H 0PT

Tel: 020 7941 7600
Fax: 020 7941 7703

www.crossrail.co.uk

CROSS LONDON RAIL LINKS LTD

CROSSRAIL LINE 1

**SETTLEMENT ESTIMATION
PROCEDURE: BOX EXCAVATIONS
AND SHAFTS**

November 2007

REVISION B

GEOTECHNICAL CONSULTING GROUP

52A Cromwell Road
London SW7 5BE
United Kingdom

Tel: +44 (0) 20 7581 8348
Fax: +44 (0) 20 7584 0157
Email: admin@gcg.co.uk

CROSS LONDON RAIL LINKS LTD**CROSSRAIL LINE 1
SETTLEMENT ESTIMATION PROCEDURE: BOX EXCAVATIONS AND
SHAFTS**

November 2007

REVISION B

TABLE OF CONTENTS	Page No.
Nomenclature	3
1. Introduction.....	4
2. Box Induced Ground Movement.....	5
2.1. Settlement.....	5
Maximum Settlement.....	8
Extent of Settlement Trough.....	8
Settlement Distribution	9
Influence Zone of Superficial Deposits	10
2.2. Horizontal Movement	10
3. Shaft Induced Settlement	13
3.1. Settlement.....	14
Maximum Settlement.....	14
Extent of Settlement Trough.....	14
Settlement Distribution	15
Influence Zone of Superficial Deposits	16
3.2. Horizontal Soil Movement.....	16
4. Building Distortion Assessment.....	16
4.1. Damage Categories Associated with Box Excavation	17
Short Building	17
Long Building.....	17
Varying Building Length.....	18
4.2. Damage Categories Associated with Shaft Excavation	20

5. Application..... 20

5.1. Implementation..... 20

5.2. Irregular Shapes 21

 Different Excavation Depths 21

 Combination of Boxes..... 22

 Convex (re-entrant) Corners..... 22

5.3. Horizontal Strain in Vicinity of Corners 23

6. Discussion..... 24

7. References..... 25

Figures 27

Nomenclature

E	Zone of influence of settlement trough, measured from wall
$\epsilon_{h,x}$	horizontal strain
H_e	Excavation depth
H_b	Building height
i	Distance of point of inflection from tunnel centre line
K	Settlement trough width parameter
L	Building length
$S_{v,max}$	Max. settlement at excavation wall
$S'_{v,max}$	Max. settlement above centre line of equivalent tunnel
$S_{h,max}$	Max. horizontal displacement at excavation wall
x	Distance from box/shaft wall
x'	Distance from centre line of equivalent tunnel
z_0	Depth of equivalent tunnel

1. Introduction

The estimation of ground movements associated with the construction of deep excavations (i.e. basement box excavations and shafts) is an important part of the design process for tunnel construction projects. On the Crossrail Line 1 project a large number of such structures are proposed both at station locations and for intermediate intervention / ventilation shafts. The geometry (plan size and depth) of these excavations differs significantly from those in published case histories.

In contrast to tunnel induced settlement, there is no commonly accepted methodology to estimate the settlement around deep excavations. Furthermore, there are only a limited number of published case studies, particularly for circular shafts.

This report reviews the available case history data and sets out the approach to be adopted for estimation of shaft and box induced ground movements in Phase 1 and 2 building damage assessments for the Crossrail Line 1 project. The parameters given are intended to be conservative, in line with the volume loss assumptions for tunnels in the first two phases of the assessment process. It will be necessary to produce a less conservative methodology for Phase 3 assessments; it is envisaged that this will be based on parametric studies using 3D finite element modelling. Alternatively, 3D finite element analyses could be undertaken for each specific location.

For the purposes of this report only vertical circular structures are referred to as shafts; all other excavations are referred to as “box excavations”. Inclined escalator “shafts” are to be treated as tunnels.

In this revision of the report, a number of typos have been corrected, particularly those that have been found in equations since the issuing of the Revision A.

2. Box Induced Ground Movement

2.1. Settlement

Figure 1 shows settlement data for a wide variety of case studies in stiff clay, including the data presented in the report “Embedded retaining walls: guidance for economic design” (CIRIA (2002)). A full list and details of the case studies can be found in Table 1. In this diagram both settlement and distance (from the wall) are normalised against excavation depth H_c . The graph shows a large scatter of settlement data with some case studies exhibiting heave close to the wall. The CIRIA report gave two “bounds” to the data presented therein (which are also shown on Figure 1) for “high” and “low” stiffness support systems of the excavation wall. The high stiffness bound has a maximum settlement of approximately $0.075\%H_c$ which develops at a distance of approximately $0.5H_c$ from the wall. The full data set shown on Figure 1 includes a high number of results within one excavation depth, H_c , which lie outside the high stiffness bound, although the data would be categorised as high stiffness. For support systems with a low stiffness (normally restricted to cantilevers or walls with a single low-level prop) the design line shows its maximum settlement of $0.35\%H_c$ at the excavation wall.

The case studies in Figure 1 include a wide variety of different box geometries, ranging from long cuttings for road underpasses to excavations for deep basements. Figure 2 compares the geometry (length, L, width, B, and depth, H_c) of these excavations with those planned for Crossrail Line 1 by plotting the aspect ratio in plan L/B (defined in the figure) against the excavation depth to plan size ratio (H_c/\sqrt{LB} i.e. depth over the square root of the plan area). The figure shows that most of the proposed Crossrail excavations and shafts have a plan aspect ratio of 2 or lower and are relatively deep compared to their plan dimensions. The case studies included in Figure 1, in contrast, can be distinguished into two groups: (1) long excavations for road works which can be interpreted as ‘plane strain’ cases, i.e. a large plan aspect ratio with a relatively shallow excavation depth; and (2) excavations for deep basements which have a low plan aspect ratio but are shallow compared to their plan dimension.

	Wall type	Construction sequence/support system	Retained soil stratigraphy	Depth	Reference
New Palace Yard	DW	Top-down, multi propped	10m of made ground/sand and gravel over London Clay	66x50 x18.5	St John (1975); Burland and Hancock (1977); Burland, Simpson & St John (1979)
YMCA	DW	1 anchor, propped by floors top-down	7.5m of made ground and gravel	45x70 x16	St John (1975); Burland et al. (1979)
British Library					
Victoria Embankment	SPW	Props and Berm	Fill and Alluvium overlying London Clay	6.5	St. John et al.
Aldersgate	DW		8m of fill over 4m of sand and gravel over London Clay	75x120 x23	Fernie at al. (1991)
A406/A10 Junction	DW counterfort	Low-propped	2.4m of made ground over London Clay		Carder et al. (1991)
Bell Common	SPW	Top-propped	7m Older Head and Claygate Beds over London Clay	PS 8	Tedd et al (1984); Symons and Tedd (1989)
Britanic House	DW	Supported by berm during excavation of central area, temporary struts, then floor cast	2.5m of sand and gravel over London Clay	150x50 14 to 20	Cole and Burland (1972); Burland at al. (1979)
East of Falloden Way (1)	CPW	Cantilever	23m of glacial till over London Clay		Brookes and Carder (1996)
East of Falloden Way (2)	DW	Cut and Cover	21m of glacial till over London Clay		Brookes and Carder (1996)
Limehouse Link	DW	Tunnel portal, cantilever	6m of made ground and terrace gravel over London Clay.		Moran and Laimbeer (1994)
Lion Yard	DW	Top-down, multi-propped	Gault Clay overlain by 3m of made ground and gravel	65x45 10	Lings et al. (1991)
Reading	DW	Cantilever	3m of made ground and terrace gravel over London Clay	PS 6.9	Burland et al. (1979); St John (1975); Carder and Symons (1989)
Neasden	DW	Anchored	0.5m of made ground over 30m of London Clay	PS 8	Sills et al (1977); Simpson et al. (1979); St John (1975); Carswell et al (1991)
Rayleigh Weir	CPW	Low-propped	3m of made ground over London Clay		Darley et al. (1994)
Walthamstow (2)	DW counterfort	Low-propped	London Clay to surface		Carder et al. (1994)
Walthamstow (1)	CPW	Top-propped	1.5m of made ground over London Clay		Carswell et al. (1993); Watson and Carder (1994)

Table 1: Summary of case studies from literature review

Thus, since the deep excavations for building developments in Central London have a similar plan aspect ratio, they are more comparable to the Crossrail geometries and this report will concentrate on these case studies, namely:

- New Palace Yard underground car park (18.5m deep);
- YMCA, Tottenham Court Road, London (16m deep);
- British Library (24m deep);
- 60 Victoria Embankment, London (19m deep);
- Aldersgate (23m deep).

The settlement measurements from these cases are shown in Figure 3. The data still show a relatively large scatter reflecting variations in shape, wall and prop stiffness, ground conditions and the effects of existing adjacent structures. Maximum values of settlement for each case occur close to the excavation, with a maximum of 0.16% H_c (for Victoria Embankment). The figure indicates that negligible settlement occurs beyond a distance of approximately $2.5H_c$. The figure includes the two curves reproduced from the CIRIA report, based on “high” and “low” support stiffness. Comparing the settlement data with these upper bounds shows that beyond a distance of $1H_c$ the data lie within the boundary for a high support stiffness. However, many data points closer to the wall exceed this boundary.

The solid line represents the proposed settlement distribution to be adopted for Phase 1 and 2 assessments. Within a distance of $1H_c$ from the wall most data points lie within this boundary. Beyond $1H_c$ the measurements coincide well with the proposed settlement profile.

There are insufficient data to justify any specific form for the settlement trough and linear, parabolic and Gaussian distributions have been proposed and used in the past for settlement assessment. The solid line in Figure 3 is defined as the hogging section of a Gaussian error function. Adoption of this form of curve is conservative since it gives higher distortions than linear or parabolic relationships. It also has the advantage that it is used for tunnel induced

settlement predictions and therefore provides a similar model for both tunnels and boxes. Figure 4 shows the definition of the settlement distribution relative to the wall position and indicates the location of an equivalent tunnel which would give the same settlement distribution (note that the equivalent tunnel is normally at a relatively shallow depth). It can be seen that the point of inflection which defines the boundary between sagging and hogging zones lies on the excavation wall, i.e. only the hogging zone is used.

The following parameters will be adopted to define the shape of the settlement trough:

$S_{v,max}$: Maximum Settlement at excavation wall

E: Extent of influence of settlement trough

These parameters are discussed in the following sections.

Maximum Settlement

The proposed settlement distribution plotted as a solid line in Figure 3 has a maximum value of 0.18% of H_c . It can be seen that most data points lie above the settlement curve. However, the upper bound line for low stiffness support systems indicates that much higher values of settlement can occur around excavations if no effective support is provided. The value of $S_{v,max}$ therefore depends on the wall support stiffness. To take account of this effect, it is proposed to use $S_{v,max} = 0.18\%$ (of H_c) for systems of high stiffness and twice this value (i.e. 0.36%) for systems of low stiffness. The low stiffness value should only be used for cantilever walls or in locations where there are no significant structures within the zone of influence.

The proposed curve for stiff support systems is deemed to allow for wall installation effects which need not be considered separately at Phase 1 or 2.

Extent of Settlement Trough

Figure 3 shows that significant settlements only develop within a distance of $2.5H_c$ from the excavation. The data in Figure 1 indicate little change in the

extent of the settlement trough with changing stiffness of the support system. It is therefore proposed to consider an extent of the settlement trough of $E = 2.5H_c$ regardless of the support system. This value is lower than the $3.75H_c$ recommended in the CIRIA report which is conservative in terms of distortions since the settlements are concentrated in a smaller zone.

The settlement assessment for tunnels only considers ground movements within the boundaries of $2.5i$, where i is the distance to the point of inflection. In the case of a box, the zone of influence is defined by $2.5H_c$. Considering that the distance of $2.5H_c$ only comprises the hogging zone of the settlement trough (which in the tunnel case has a length of $1.5i$) it is:

$$E = 3/2i = 5/2H_c \quad (1)$$

as illustrated in Figure 4.

Settlement Distribution

Figure 4 shows that two coordinate systems can be used to describe the settlement equation:

- x describes the distance from the excavation wall;
- x' describes the distance to the centre line of an equivalent tunnel.

The relationship between the coordinate systems is:

$$x' = x + i \quad (2)$$

$S_{v,max}$ and $S'_{v,max}$ are maximum settlement values corresponding to the x and x' coordinates as shown in Figure 4. The settlement curve is described by the following equation:

$$S_v(x') = S'_{v,max} e^{-\frac{x'^2}{2i^2}} \quad (3)$$

which is equivalent to the Gaussian settlement curve commonly adopted for tunnel induced settlement (Attewell et al., 1986). Using the x -coordinate system it can be expressed as:

$$S_v(x) = S_{v,\max} e^{\frac{1}{2}} e^{-\frac{(x+i)^2}{2i^2}} \quad (4)$$

since $S_{v,\max} = S_{v,\max}^2 e^{-1/2}$. Substituting

$$i = \frac{2}{3} E = \frac{5}{3} H_e \quad (5)$$

leads to:

$$S_v(x) = S_{v,\max} e^{\frac{1}{2}} e^{-\frac{(x+\frac{2}{3}E)^2}{2(\frac{2}{3}E)^2}} = S_{v,\max} e^{\frac{1}{2}} e^{-\frac{(x+\frac{5}{3}H_e)^2}{2(\frac{5}{3}H_e)^2}} \quad (6)$$

Since the ratios $S_{v,\max}/H_e = 0.18$ and $E/H_e = 2.5$ are constants, it follows that the shape of the settlement curve, since both axes are normalised against excavation depth, does not depend on the box geometry. The ratio $S_{v,\max}/E$ remains constant and equal to 0.072%.

Influence Zone of Superficial Deposits

In the close vicinity of a box, the settlement can be significantly influenced by wall installation effects, local foundation details and propping arrangements in the early stages of excavation; these effects are relatively local and are usually related to the superficial deposits overlying the London Clay or Lambeth Group (i.e. Made Ground / Brick Earth / Alluvium / Terrace Gravel). Special consideration is required in the construction methodology and therefore all buildings which are located close to excavations, within a zone defined by a distance equal to the depth of superficial deposits, automatically have to undergo a Phase 3 assessment.

2.2. Horizontal Movement

Figure 5 presents data of horizontal movement induced by box excavation from the CIRIA report “Embedded retaining walls: guidance for economic design”. More details of the case studies are listed in Table 1. The scatter in this figure is comparable to that in Figure 1. Unfortunately, data of horizontal movement were not available for all case studies from the construction of deep basements shown in Figure 3. Due to the insufficient data for these box geometries, the

proposed horizontal displacement curve is compared to all case studies presented in the CIRIA report (i.e. including those with a geometry which departs significantly from those on Crossrail).

Figure 5 includes the proposed distribution of horizontal displacement for use on Crossrail, together with the upper bounds presented in the CIRIA report. The proposed distribution is derived from the Gaussian curve adopted for the settlement estimation. Assuming an equivalent tunnel centred at a depth of z_0 and a distance of i on the inner side of the excavation, it is assumed that all ground movement vectors point towards the centre of this tunnel, i.e. the same assumption as commonly applied for tunnel induced ground movement predictions. This situation is plotted in Figure 6 (note that, for clarity, the tunnel in Figure 4 was shown diagrammatically, at a greater depth). As noted for the settlement data, there are insufficient measurements available to justify a specific shape of the horizontal displacement distribution. The proposed curve shown in Figure 5 is used as it is compatible with the Gaussian curves adopted for tunnel induced settlement estimation and gives higher, and consequently more conservative, horizontal strains at distances up to $2H_c$ from the excavation.

At distances greater than $2H_c$ from the excavation retaining wall some data points exceed the boundary given by the proposed horizontal displacement curve. The majority of these points are from two case studies, New Palace Yard and Neasden. At New Palace Yard the horizontal displacement profile was influenced by substantial existing structures, i.e. the data points from this case history in Figure 5 represent, in part, rigid body movements of sections of the surrounding buildings. At Neasdon, an underpass was built with an anchored wall (see Table 1); an anchored wall tends to transmit the horizontal movement to the rear of the anchored zone, thus increasing the distance from the excavation at which movements are recorded. Thus, there are good reasons for the abnormally high horizontal movements at distance recorded in these two case studies.

Using the x' -coordinate system shown in Figure 4 the horizontal settlement can be expressed as

$$S_h(x') = -\frac{x'}{z_0} S_v(x') \quad (7)$$

with $i = K * z_0$ this can be rearranged to

$$S_h(x) = -K \frac{x+i}{i} S_v(x) \quad (8)$$

This can be written as

$$S_h(x) = -K \left(1 + \frac{3x}{2E} \right) S_v(x) = -K \left(1 + \frac{3x}{5H_e} \right) S_v(x) \quad (9)$$

At the wall (i.e. the point of inflection) the horizontal movement is $S_{h,max} = -K * S_{v,max}$ (see Figure 6) i.e.

$$K = \frac{S_{h,max}}{S_{v,max}} \quad (10)$$

For the proposed settlement distribution shown in Figure 5, a value of $S_{h,max}/S_{v,max} = 1.0^1$ was adopted. All parameters for vertical and horizontal settlement calculations are summarised in Table 2.

	$S_{v,max}$	E	$S_{v,max}/S_{h,max}$
High stiffness	0.18% H_e	2.5 H_e	1.0
Low stiffness	0.36% H_e	2.5 H_e	1.0

Table 2: Settlement parameters for box excavation.

This section has shown that box induced settlement can be estimated using similar equations to those used for tunnel induced settlement. For the conversion between the equivalent tunnel model and the box system the following relations are summarised:

¹ A ratio of 1.15 has been used to date based on parameters suggested by Mott MacDonald. This value has been reappraised in the production of this report and the value of 1.0 is preferred.

$$S_{v,\max} = S'_{v,\max} * e^{-1/2} \quad (11)$$

$$i = 2/3 E \quad (12)$$

$$K = S_{h,\max}/S_{v,\max} \quad (13)$$

$$z_0 = i/K = 2/3 E S_{v,\max}/S_{h,\max} \quad (14)$$

3. Shaft Induced Settlement

Field measurements for shaft induced settlement are rare. New and Bowers (1994) presented measurements from an access shaft for the Heathrow Express Trial tunnel in London. The shaft had a diameter of $D = 11\text{m}$ and a depth of $H_e = 26\text{m}$. They reported a maximum settlement of $0.06\%H_e$ and no significant settlement was measured beyond $1H_e$. This case study shows that for circular shafts the settlement values are reduced when compared with the case history data for large boxes. This behaviour is confirmed by comparisons of axial symmetric finite element analyses with those performed in plane strain conditions (e.g. Torp-Petersen et al. (2003)). Anecdotal evidence from the Jubilee Line Extension confirms the intuitive engineering expectation that this effect would be enhanced with reducing shaft diameter; this should be taken into account in the method for estimating settlement.

The very limited case history data means that any attempt to produce a mathematical model to quantify shaft induced ground movements has to be, at least partially, based on engineering judgement. The criteria used to guide the model described herein are:

- For consistency, settlements and horizontal movement distributions should be based on the Gaussian equations used for boxes and tunnels;
- For shafts of the same diameter, the settlement behaviour is similar to that of boxes in that the settlement curves coincide when normalised against shaft depth;
- The maximum settlement $S_{v,\max}$ and the extent of the settlement trough, E , depend on the shaft diameter D as well as the depth H_e ;

- The maximum settlement $S_{v,max}$ and the extent of the settlement trough, E , will not exceed the values for box excavations.

3.1. Settlement

Maximum Settlement

It is proposed that the maximum settlement (normalised by H_e) increases linearly with shaft diameter. The linear function is defined to be consistent with the case study by New and Bowers giving $S_{v,max}/H_e = 0.06\%$ for $D = 10\text{m}$ (which is a conservative approximation as the diameter in their case study was $D = 11\text{m}$). Therefore:

$$S_{v,max}/H_e = 0.006\% * D \quad (\text{with } D \text{ being measured in metres}) \quad (15)$$

This function would lead to high values of maximum settlement for large diameter. Therefore an upper bound is defined by

$$S_{v,max}/H_e = 0.15\% \text{ for } D > 25\text{m} \quad (16)$$

This relationship is plotted in Figure 7a. The maximum value of $S_{v,max}/H_e = 0.15\%$ is slightly smaller than that adopted for box excavations (0.18%). This smaller value is used as shaft excavations (in cohesive soils) are normally constructed by underpinning which will not produce any separate installation effect.

Extent of Settlement Trough

New and Bowers (1994) reported an extent of $1H_e$ for the 11m diameter shaft described in their study. A linear function of increasing E/H with increasing D is proposed within the limits of

$$E/H_e = 1.0 \quad \text{for } D < 10\text{m} \quad (17)$$

$$E/H_e = 2.0 \quad \text{for } D > 25\text{m} \quad (18)$$

The variation between $D = 10$ and 25m can be expressed by the following equation:

$$E/H_c = 1.0 + (D-10.0)/15 \quad (\text{with } D \text{ being measured in metres}) \quad (19)$$

This relationship is illustrated in Figure 7b.

Settlement Distribution

The hogging section of the Gaussian settlement distribution (as adopted for boxes) is applied to estimate shaft induced settlement with appropriate values of $S_{v,max}$ and E being summarised in Table 3.

Situation	$S_{v,max}/H$ [%]	Extent / H [-]	S_h/S_v
$D < 10\text{m}$	0.006 D	1.0	1.0
$10\text{m} < D < 25\text{m}$		$1.0 + (D-10.0)/15$	1.0
$D > 25\text{m}$	0.15	2.0	1.0

Table 3: Parameters for shaft calculation. *Note: Diameter being measured in metre*

Figure 8 presents the data from New and Bowers (1994) and with the parabolic settlement prediction proposed by these authors which varies between 0.06% H_c at the shaft wall (zero distance) and zero at a distance of $1H_c$ from the shaft. There is data from two instrumented section lines, extending radially from the shaft. The proposed settlement curve using a Gaussian curve has been added to Figure 8. This curve is also based on a maximum settlement of 0.06% H_c and an extent of settlement equal to $1H_c$ from the shaft. In this case there is a finite settlement at a distance of $1H_c$ since the method of fitting the Gaussian curve gives 7% of the maximum settlement at the distance defined as the extent of the settlement zone.

It can be seen from Figure 8 that the New and Bowers' equation gives a good fit to the "T-line" measurements whereas the proposed Gaussian curve is more conservative and, incidentally, fits the data points on the "S-line" more accurately. The differences are small and it is concluded that it is justified to adopt a Gaussian distribution.

Influence Zone of Superficial Deposits

For the reasons discussed in Section 2.1 in relation to box excavations, a zone in the immediate vicinity of shafts is defined where a Phase 3 assessment is required; i.e. buildings within a plan distance equal to the thickness of superficial deposits of a shaft, require a Phase 3 assessment.

3.2. Horizontal Soil Movement

The field measurements of horizontal soil movement presented by New and Bowers (1994), reproduced in Figure 9, show a wide scatter and no trendline was fitted to these data by the authors. However, the data indicate that the maximum horizontal ground surface movement is similar or smaller in magnitude than observed settlement.

For estimating the shaft induced horizontal ground movement, the same approach as outlined for box excavations is adopted with the ratio of maximum horizontal to vertical settlement being $S_{h,max}/S_{v,max} = 1.0$ for all shaft diameters D .

Table 3 summarises the parameters adopted for shaft induced settlement estimation. The proposed curve is plotted in Figure 9 and it can be seen that close to the shaft it corresponds to the measurement of the S-Line, but significantly over-estimates the more well-conditioned data from the T-line.

4. Building Distortion Assessment

The previous section described the ground movement estimation procedure for boxes and shafts. In this methodology the settlement trough due to boxes depends only on the excavation depth, H_e , whilst for shafts it also depends on the shaft diameter, D . This section investigates the implications of these assumptions when applying the method to a building distortion assessment.

4.1. Damage Categories Associated with Box Excavation

Short Building

For very short buildings the average horizontal strain (which is used in the Phase 2 assessment) becomes, in the limit, equivalent to the ‘tangent’ strain, calculated for the ‘point’ at which the building is located. For tunnels the maximum value of horizontal tensile strain occurs at a distance of $x' = \sqrt{3}i$ from the tunnel centre line (x' is the local coordinate system associated with the equivalent tunnel, shown in Figure 4). The settlement at this position is:

$$S_v(x' = \sqrt{3}) = S'_{v,\max} e^{-\frac{3i^2}{2i^2}} = S'_{v,\max} e^{-\frac{3}{2}} \quad (20)$$

The transverse horizontal strain distribution caused by a tunnel is given by:

$$\varepsilon_{h,x}(x') = \frac{S_v(x')}{z_0} \left(\frac{x'^2}{i^2} - 1 \right) \quad (21)$$

The horizontal strain at $x' = \sqrt{3}i$ can be calculated as:

$$\begin{aligned} \varepsilon_{h,x}(x' = \sqrt{3}i) &= \frac{S'_{v,\max} e^{-3/2}}{\frac{2}{3} E S_{h,\max} / S_{v,\max}} (3 - 1) = 3 \frac{S_{v,\max}}{S_{h,\max}} \frac{S_{v,\max} e^{1/2} e^{-3/2}}{E} \\ &= 3 \frac{S_{v,\max}}{S_{h,\max}} \frac{S_{v,\max} / H}{E / H} e^{-1} \\ &= 3 * 1.0 * \frac{0.18/100}{2.5} e^{-1} = 0.079\% \end{aligned} \quad (22)$$

Long Building

For a long building, the average strain is calculated from the difference in horizontal displacement at the two edges of the building (or the boundaries of the sagging / hogging zones) divided by the corresponding length. If a long building spans over the entire zone of influence, from the wall to a distance of $2.5H_e$, the edges of the building experience the following displacement values at the wall and at a distance of $2.5 H_e$ from the wall respectively (note that $x = 2.5 H_e$ is equivalent to $x' = 2.5i$):

$$S_h(x'=i) = \frac{S_{h,\max}}{S_{v,\max}} S_{v,\max} \quad (23)$$

and

$$S_h(x'=2.5i) = \frac{S_{h,\max}}{S_{v,\max}} S_{v,\max} 2.5e^{1/2} e^{-2.5^2/2} = \frac{S_{h,\max}}{S_{v,\max}} S_{v,\max} 2.5e^{\frac{1-2.5^2}{2}} \quad (24)$$

The average horizontal strain can then be calculated as the difference of Equations (23) and (24) divided by the length of the zone of influence $E = 2.5H_e$:

$$\frac{S_h(x'=i) - S_h(x'=2.5i)}{E} = \frac{S_{h,\max} / S_{v,\max} S_{v,\max} \left(1 - 2.5e^{\frac{1-2.5^2}{2}}\right)}{E} = 0.0590\% \quad (25)$$

Since the ratio $S_{v,\max}/E$ is independent of H_e , the hogging deflection ratio for a structure spanning over the entire hogging zone (defined by the point of inflection and the end of the zone of influence) can be shown to be $0.07265 S_{v,\max}/i$. Substituting $S_{v,\max}$ and i leads to:

$$DR_{hog} \approx 0.07265 \frac{S_{v,\max}}{i} = 0.07265 S_{v,\max} e^{-1/2} \frac{3}{2E} = 0.0130\% \quad (26)$$

Varying Building Length

It has been shown that the values of horizontal strain and deflection ratio are independent of the dimensions of the box. This is due to the normalisation of both the maximum settlement, $S_{v,\max}$, at the wall and the extent, E , of the settlement curve against the excavation depth H_e . Thus, for increasing H_e , the settlement curve is scaled up. Consequently the shape of the curve (settlement and horizontal displacement) remains constant, leading to constant values of horizontal strain and deflection ratio regardless of the value of H_e .

However, the distortion of a building depends on its length compared to the extent of the settlement curve, i.e. compared to $2.5H_e$. The length above which a building covers the entire hogging zone is defined by $L \geq 2.5 H_e$.

The influence of building length can be illustrated on an interaction diagram, plotting deflection ratio against horizontal strain, for a range of different building lengths and excavation depths. Figure 10 shows an interaction diagram with data sets for two excavation depths of $H_e = 10$ and 30m. For each depth the same range of building lengths was considered ($L = 4, 8, 16, 24, 32, 40, 48$ and 90m). The maximum value (90m) is longer than the settlement trough of the deeper excavation ($2.5H_e = 75\text{m}$); i.e. this case covers the entire hogging zone. For both data sets Figure 10 shows a similar pattern of horizontal strain reducing with increasing building length, L , while the hogging deflection ratio increases with decreasing L . It can be seen that both data sets follow the same path. For $L \rightarrow 0$, the horizontal strain equals 0.079% (from Equation 22) with zero deflection ratio, whereas for $L > 2.5 H_e$, a horizontal strain of 0.059% is obtained (Equation 25) together with a hogging deflection ratio of 0.013% (Equation 26).

Ratios of L/H_e are indicated on Figure 10 which show that for $L/H_e = 0.8$ the data points for $H_e = 10\text{m}$ ($L = 8\text{m}$), and $H_e = 30\text{m}$ ($L = 24\text{m}$), coincide. Similarly, for $L/H_e = 1.6$ the 16m long building for $H_e = 10\text{m}$ and the 48m long building with $H_e = 30\text{m}$ give the same result. In the $H_e = 10\text{m}$ analysis the full hogging zone is covered for buildings of $L \geq 25\text{m}$, while for the 30m deep excavation this condition is reached for $L \geq 75\text{m}$ (i.e. this situation only arises for the 90m long building). Thus, the distance between the data points is smaller in the $H_e = 30\text{m}$ analysis.

Figure 11 shows the same data plotted to a different scale in order to include the boundaries of the damage categories; the boundaries are shown for building length to height ratios (L/H_b) of 1 and 4. The figure demonstrates that the deformation states of the buildings analysed fall close to the lower boundary of a potential damage category 2 ('slight') for which no further investigation is required. The maximum possible value of tensile building strain for structures affected by settlement from a single box excavation is 0.08%; thus, a Phase 3 assessment is only required for buildings close to excavations or where there is a combined effect from tunnels and boxes.

4.2. Damage Categories Associated with Shaft Excavation

Section 4.1 demonstrated that the maximum value of potential building strain, which can develop within the settlement trough of a box, is independent of the depth of the box. This principle also applies to shafts, but only for a given diameter since, for shafts, the settlement trough is also affected by the shaft diameter.

A similar study of the effect of shaft excavation on potential damage to buildings of varying length was performed. For a given shaft diameter the result was similar to that from the box study; i.e. the value of maximum potential tensile building strain for a variety of building geometries affected by shaft construction was independent of the shaft depth. This maximum building strain value, however, depends on the shaft diameter D as shown in Figure 12. For large diameters, i.e. $D > 25\text{m}$ the maximum potential building strain is 0.08% and does not increase further as D increases. This value is effectively identical to that calculated for box induced settlement (the effect of reduced maximum settlement and reduced trough width cancel each other). As D decreases, the maximum potential strain reduces. Between $D = 10$ and 25m there is a non-linear relation between the maximum potential building strain and the diameter. This is due to the dependence on diameter of both $S_{v,\max}$ and E . For $D < 10\text{m}$ the curve is linear, since only $S_{v,\max}$ depends on diameter, whilst E is independent of the diameter.

5. Application

5.1. Implementation

The proposed settlement estimation procedure for boxes and shafts is relatively easy to implement. For a grid of surface points, the distance of every grid point to the excavation wall must be calculated. This is straightforward for a circular shaft. For a box with corners the shortest distance between each surface point and the wall must be determined. The horizontal movement of each surface point is directed towards the closest point of the wall. Figure 13 shows this situation for a rectangular box. In the vicinity of the corners, the horizontal movement vectors point in a radial direction towards the corner, whilst along the

walls the vectors are perpendicular to the wall. One possible method of determining the shortest distance between a given point and the wall is to identify different zones around the corners and along the walls, as indicated in Figure 13². Figure 14 shows contours of settlement calculated using this approach for a 10 x 40m box with a depth of 20m. It can be seen that the contour lines run parallel within the influence zone of each wall. Figure 15 shows the corresponding contour plot of horizontal soil movement. The contour lines refer to maximum scalar value of horizontal displacement. The plot is overlain with vectors of horizontal soil movement which indicate that the movement always points towards the closest point of the excavation retaining wall.

5.2. Irregular Shapes

The method of estimating settlement due to box excavations is not limited to a specific shape for the box, however, in practice a limit might be set on the number of corners in a settlement program. Boxes may also have zones of different excavation depths. In many cases it is possible to adequately represent boxes with complex shapes by a simple quadrilateral shape which can be easily analysed by applying the above described procedure. Engineering judgement is required, bearing in mind that areas in close proximity to the box have to undergo a Phase 3 assessment in any case.

In other cases, however, such a simplification might not be appropriate. This section describes how to deal with more complex box geometries.

Different Excavation Depths

A single box excavation can include areas with different excavation depths. To estimate the settlement the box can be modelled by superimposing the settlements due to different parts of the box. Figure 16 shows such a situation. Firstly, the entire box area is analysed applying the minimum value of excavation

² This method is of course not restricted to quadrilateral boxes. The same approach could be adopted for boxes with more corners. For simplicity only the case of four corners will be discussed here.

depth. In the second stage the area of the deep excavation is modelled and the settlement from this calculation is added to the results from the first (i.e. shallow) box. By applying this procedure, the upper part of the deep box is modelled twice and the settlement from this part must therefore be subtracted from the previous sum of settlements.

Combination of Boxes

Boxes of irregular shapes or with a high number of corners can be modelled by combining a number of regular shaped boxes. Figure 17 shows such a situation. Two four-corner boxes are combined to model a five corner box. In this example it is assumed that the excavation depth is constant over the entire box. The wall which connects both sub-boxes (referred to as box 1 and 2) must not contribute to the settlement calculation. This can be achieved by calculating the shortest distance from any surface point to the walls of both boxes separately and then adopting the smaller of the two; this will give the minimum distance to the wall of the entire box of every surface point. Using this distance, the settlement and horizontal displacement can be calculated using the above described approach. The direction of horizontal movement is defined by the vector associated with this minimum distance.

Figure 18 shows the results of a calculation for a five corner box. The black contour lines represent contours of settlement for a five corner box. It can be seen that within the influence zone of each wall the contour lines run parallel to the wall. If the settlement was calculated by simply adding the settlement of both boxes, larger values of settlement would occur as indicated by the orange dotted contour lines. These lines do not run parallel to any of the walls. The reason for this behaviour is that by treating both boxes independently the wall between the two boxes also contributes to the settlement – clearly an unrealistic assumption.

Convex (re-entrant) Corners

The boxes illustrated in Figures 17 and 18 only have concave corners (i.e. internal angle $< 180^\circ$). The situation of a box with a convex, re-entrant corner is shown in Figure 19. The same approach as outlined above for irregular shaped boxes can be adopted, i.e. calculating the minimum distance between any surface

point and the wall of the excavation. However, it has to be noted that in vicinity of the convex corner (bottom left hand side in the figure) such an approach can predict high tensile strain due to opposite horizontal movement components associated with the two adjacent box walls. In addition, for this geometry both of the adjacent wall deflections would be expected to contribute to settlement. A conservative approach should be adopted, for example, an approximation of the box geometry as shown in Figure 20 could be used in order to overcome these problems. Engineering judgement is required to determine a suitable model for analysis, or alternatively, to define an enlarged area local to the re-entrant corner for more detailed consideration in a Phase 3 assessment.

A more refined methodology or site specific numerical analyses will be required for Phase 3 assessments.

5.3. Horizontal Strain in Vicinity of Corners

High values of horizontal strain can be calculated on section lines in the vicinity of the corners of a box. Figure 21 shows a section line running parallel to a wall of a rectangular box and extending beyond one of the corners. In the part of the section line which runs parallel to the wall there is no horizontal movement in the longitudinal direction of the section as all horizontal displacement vectors point towards the wall, i.e. perpendicular to the section. As the section line enters the zone beyond the corner of the box, this situation changes and the movement vectors are directed towards the corner of the box producing a component of horizontal displacement in the direction of the section line. Within a relatively short distance from the corner, relatively large horizontal movements along the section line can develop, leading to high values of horizontal compressive strain in this area. With increasing distance, the absolute value of horizontal displacement decreases leading to a zone of tensile strain, as shown schematically in Figure 21. Figure 22 presents results of a calculation for such a situation; the section which runs parallel to the long axis at a distance of 5m from a 40m long (and 10m wide) box of 20m excavation depth. Negative values indicate movement towards the box. The rapid increase of horizontal axial movement along the section (producing compressive strain) is given over a distance of 10m

beyond the corner (longitudinal coordinate 0 to approximately 10m). Tensile horizontal strain is given between 10 and 100m.

6. Discussion

This report presents the method to be used to estimate ground movement induced by deep box excavations and shafts in Phase 1 and 2 assessments.

A limited number of field studies are available for deep excavations in London Clay and, since these differ in the size of the excavation, the support stiffness or the urban environment, there is a relatively large scatter in the results. As a result, upper bound curves have been fitted to the data in the past (e.g. CIRIA, 2002) instead of providing design lines.

The approach outlined in this report establishes a set of equations to estimate the ground movements around boxes and shafts. To take account of the small number of field data, the settlement profiles described herein are intentionally conservative. To this end, a Gaussian distribution of both settlement and horizontal displacement was selected; this has the added benefit of being consistent with the approach used to estimate tunnel induced settlement. The settlement trough is described as the hogging part of the Gaussian curve, i.e. the point of inflection is located at the box or shaft wall. After defining the extent of the curve, the horizontal movement can be derived assuming all vectors of movement are directed to the centre of an equivalent tunnel.

This methodology has following advantages:

- It is consistent with the settlement assessment adopted for tunnel construction;
- It uses a simple model which can easily be implemented in engineering practice

However the model has the following drawbacks:

- The 3D geometry of boxes is not considered. The settlement profile along the centre line of a long excavation wall gives the same settlement profile as at the corner of the excavation. Field data, however, have

demonstrated that smaller settlement occurs around the corner where the excavation wall is effectively stiffer.

- The influence of the diameter of circular shafts is considered in the equation with reducing diameter leading to smaller settlement. However, the proposed formulation is based on very limited field data.
- The approach of normalising both maximum settlement and the distance against excavation depth H_c leads to unique normalised settlement curves for boxes and shafts (for a given diameter). This approach gives a unique value of building strain for a given ratio of building length to excavation depth L/H_c .
- The approach leads to sudden changes in the components of horizontal movement along a section line in the vicinity of corners, resulting in locally high values of compressive strain.

The requirement to develop a simple, consistent and conservative methodology based on existing knowledge was the determining factor. The building strain derived from this model is therefore likely to be over predicted, particularly for the deep, relatively small plan area boxes proposed for Crossrail. Settlement reducing effects from the influence of corners, moderate support stiffness (compared to a low stiffness) have not been addressed. It therefore has to be noted that the approach has been developed for Phase 1 and 2 settlement assessments only. It will be necessary to produce a more refined and less-conservative methodology for Phase 3 assessments. It is envisaged that this will be based on parametric studies using 3D finite element modelling. Alternatively, 3D finite element analyses could be undertaken for each specific location.

7. References

Attewell, P. B., Yeates, J. & Selby, A. R. (1986). *Soil movements induced by tunnelling and their effects on pipelines and structures*. Balckie, Glasgow.

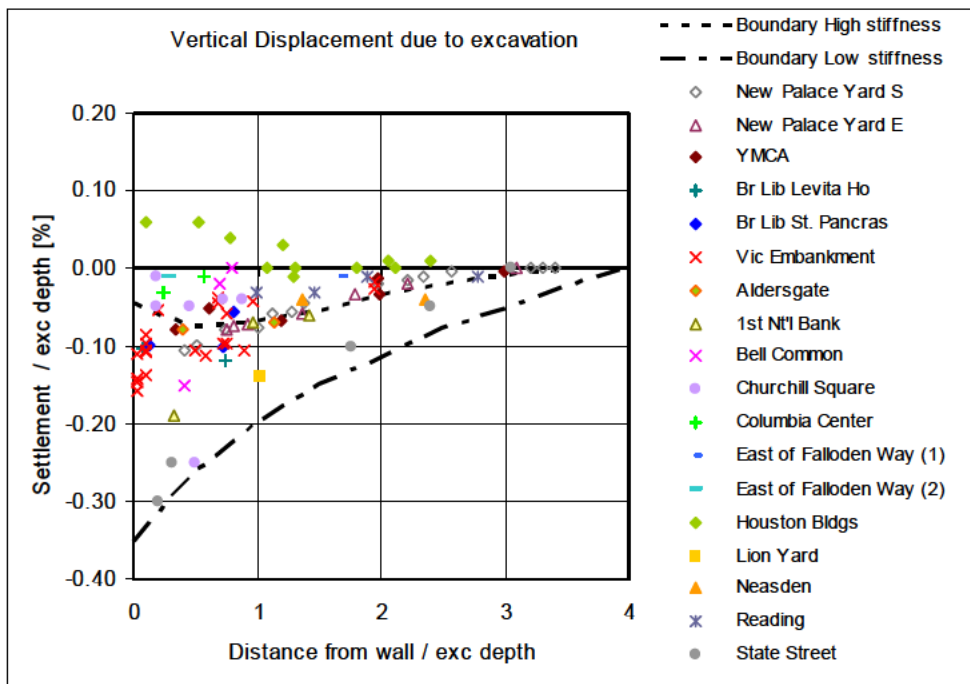
CIRIA (2002). *Embedded retaining walls: guidance for economic design*. Funders' Report CP 96, March 2002.

New, B. M., & Bowers, K. (1994). Ground movement model validation at the Heathrow Express trial tunnel. Pages 310–329 of: *Tunnelling '94*.

St John, H. D., Potts, D. M., Jardine, R. J. & Higgins, K. G. (1993). Prediction and performance of ground response due to construction of a deep basement at 60 Victoria Embankment. *Predictive Soil Mechanics, Proc. of Wroth Memorial Symposium*. Thomas Telford, London

Torp-Petersen, G., Zdravkovic, L., Potts, D.M. & St. John, H.D. (2003). The prediction of ground movements associated with the construction of deep station boxes. World Tunnelling Congress, 2003.

Figures



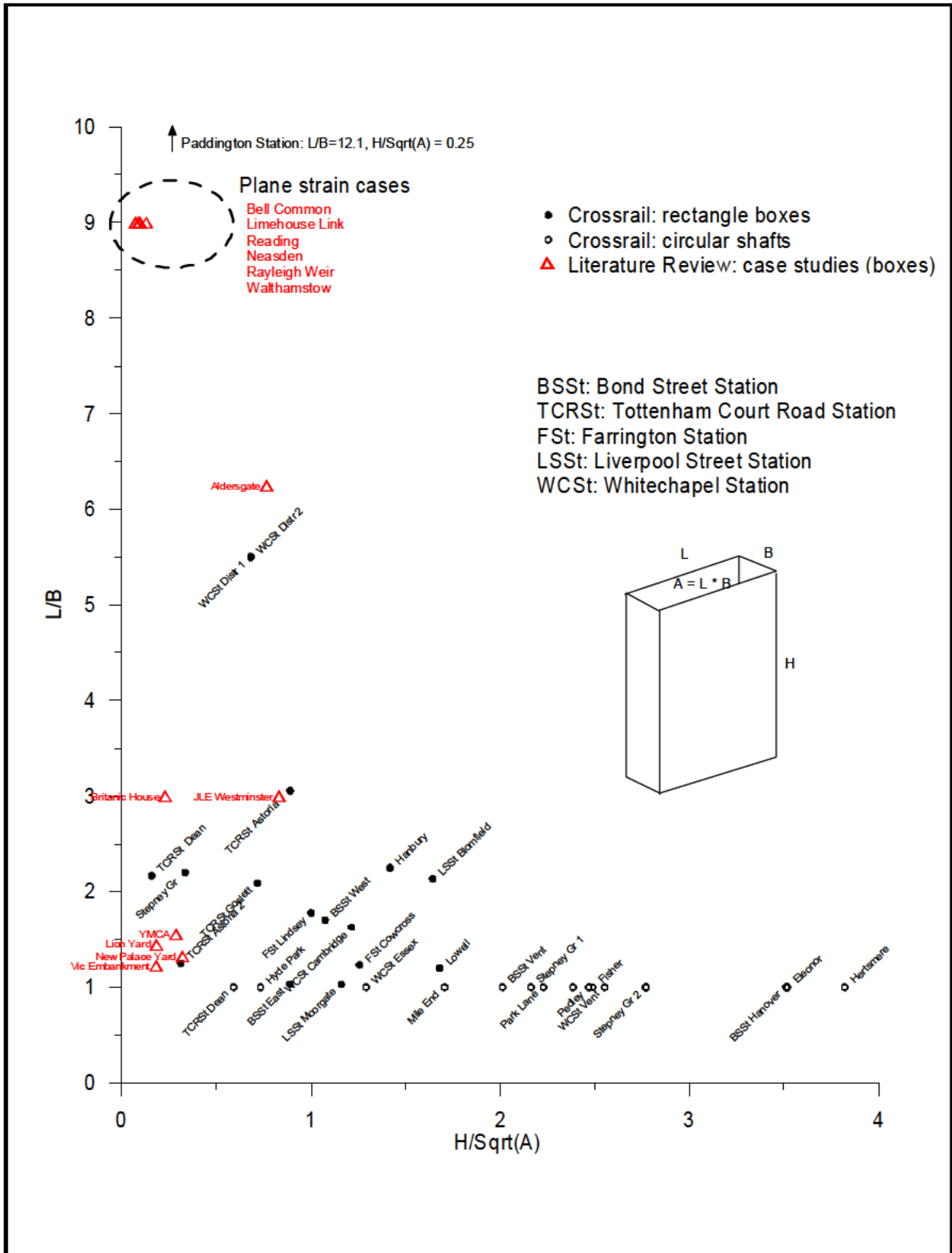
Crossrail: Settlement Estimation Procedure

Box Excavations and Shafts

Normalised settlement of case studies, (including data from CIRIA (2002))

Figure

1



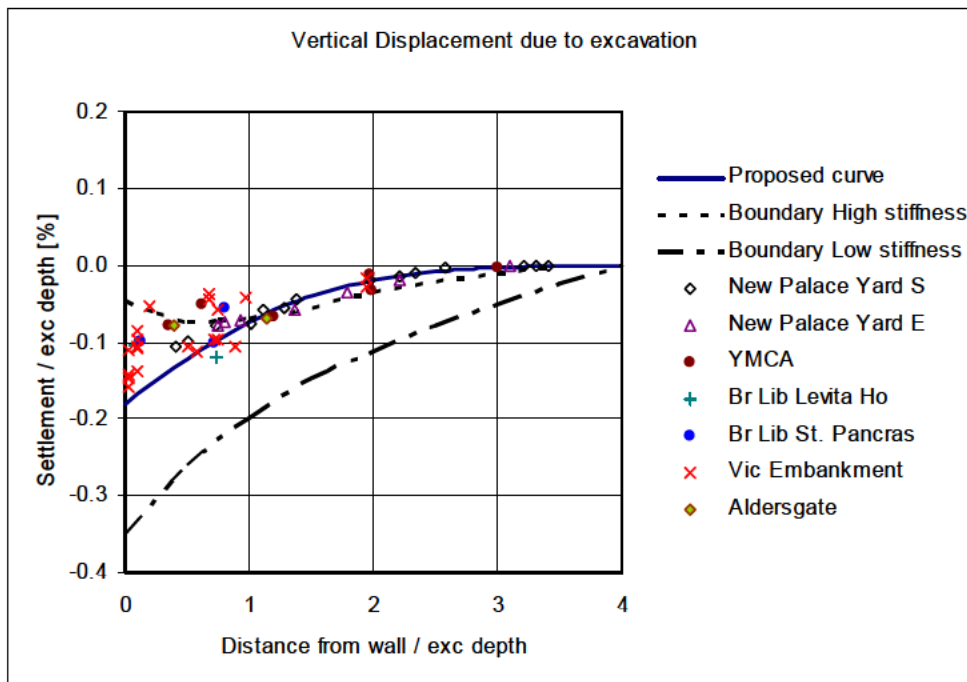
Crossrail: Settlement Estimation Procedure

Box Excavations and Shafts

Geometry of boxes and shafts from case studies compared with Crossrail cases

Figure

2



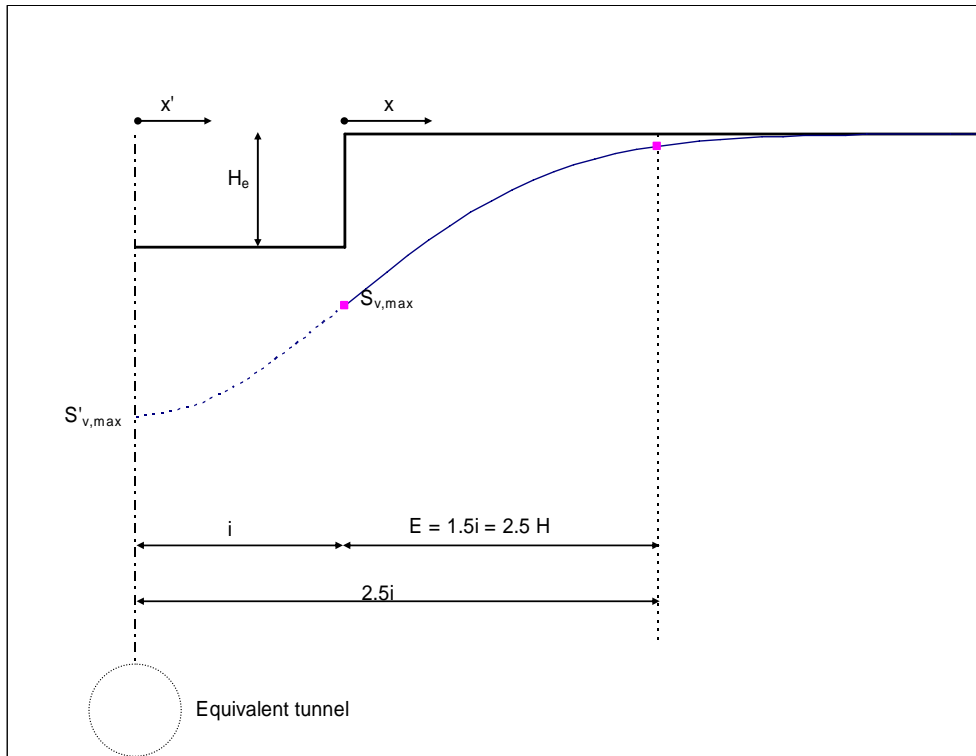
Crossrail: Settlement Estimation Procedure

Box Excavations and Shafts

Settlement of case studies (deep basement excavations only)

Figure

3



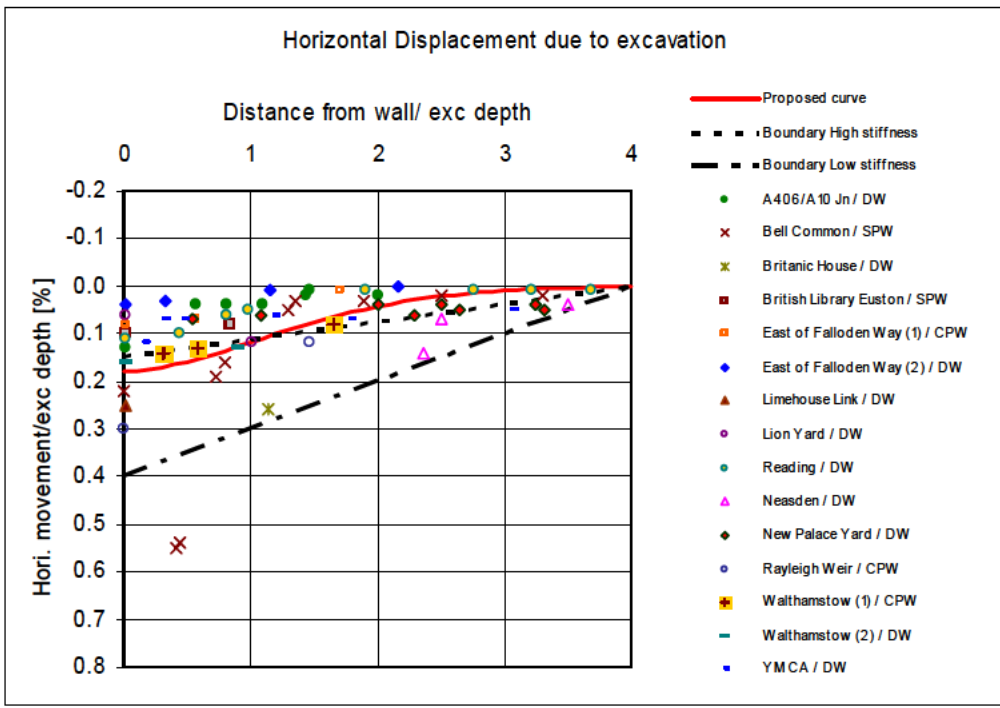
Crossrail: Settlement Estimation Procedure


Box Excavations and Shafts

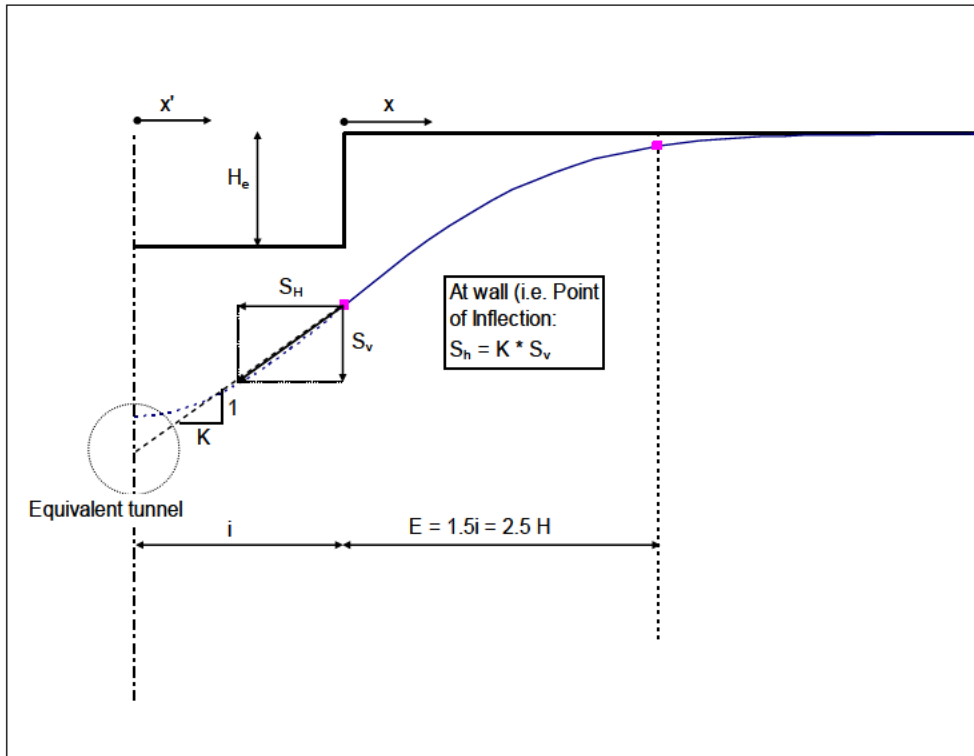
Proposed settlement behaviour due to box excavation

Figure

4



	<p>Crossrail: Settlement Estimation Procedure</p> <p>Box Excavations and Shafts</p>	<p>Figure</p> <p>5</p>
	<p>Horizontal soil movement of case studies from literature review (after CIRIA, 2002)</p>	



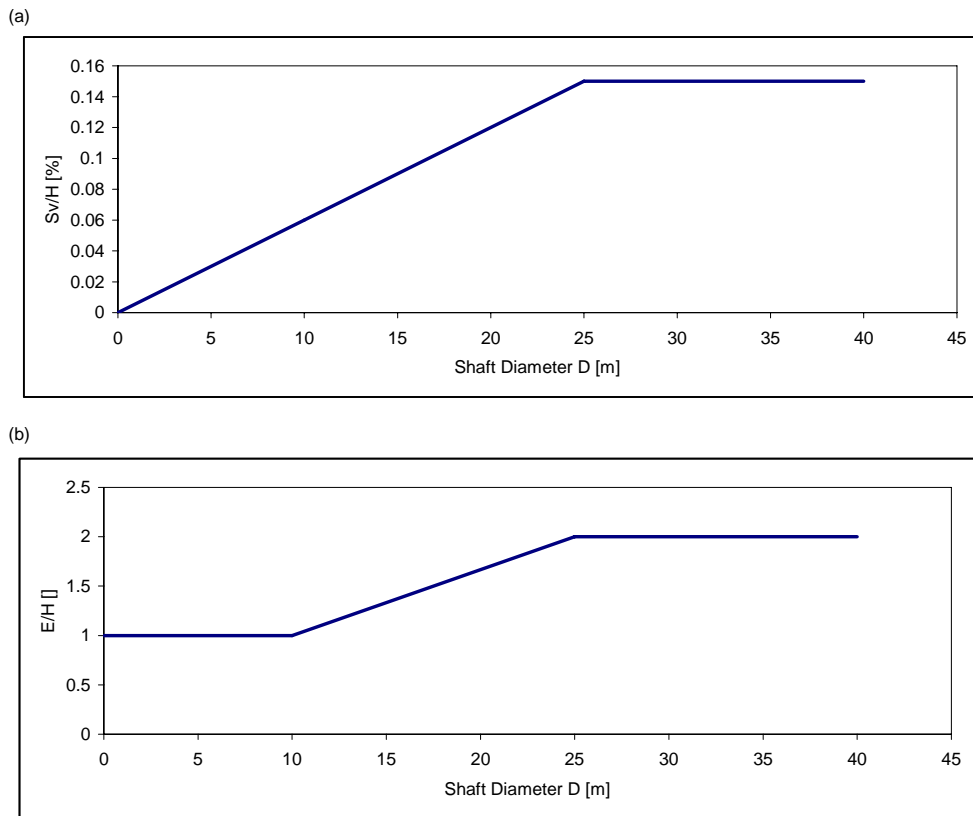
Crossrail: Settlement Estimation Procedure

Box Excavations and Shafts

Geometry of horizontal ground movement

Figure

6



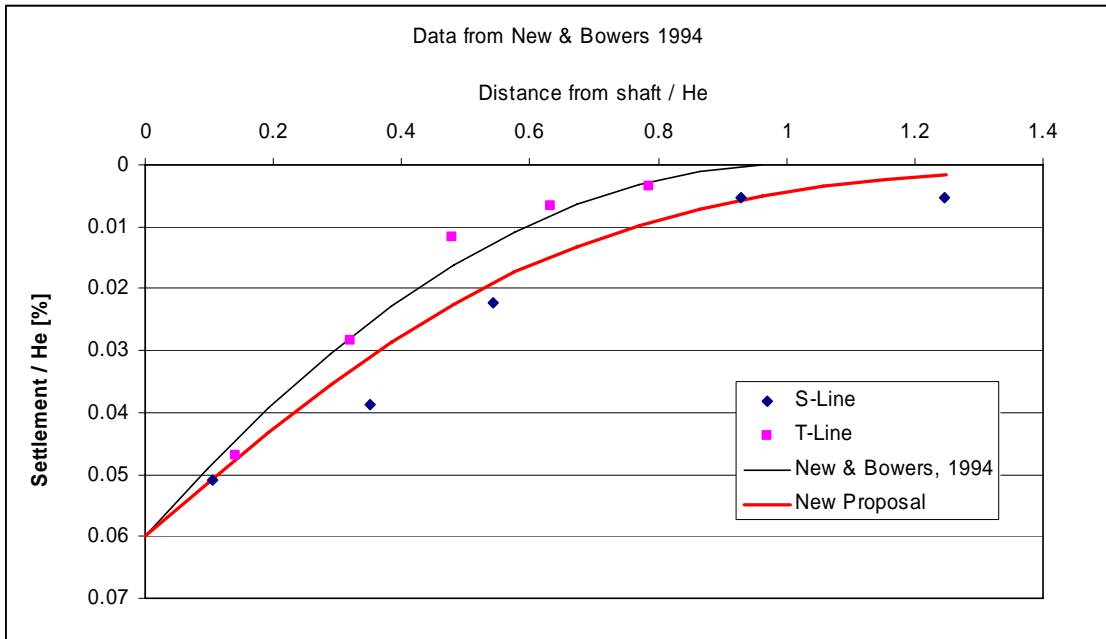
Crossrail: Settlement Estimation Procedure

Box Excavations and Shafts

Settlement parameters for shafts

Figure

7



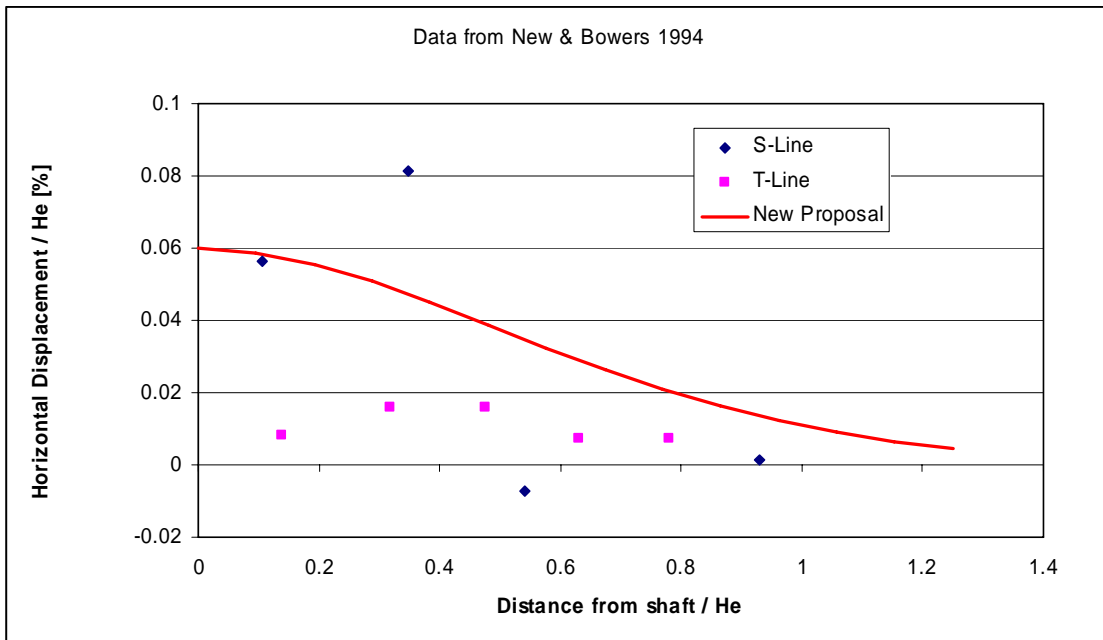
Crossrail: Settlement Estimation Procedure

Box Excavations and Shafts

Field data from New & Bowers (1994) compared with proposed settlement estimation

Figure

8



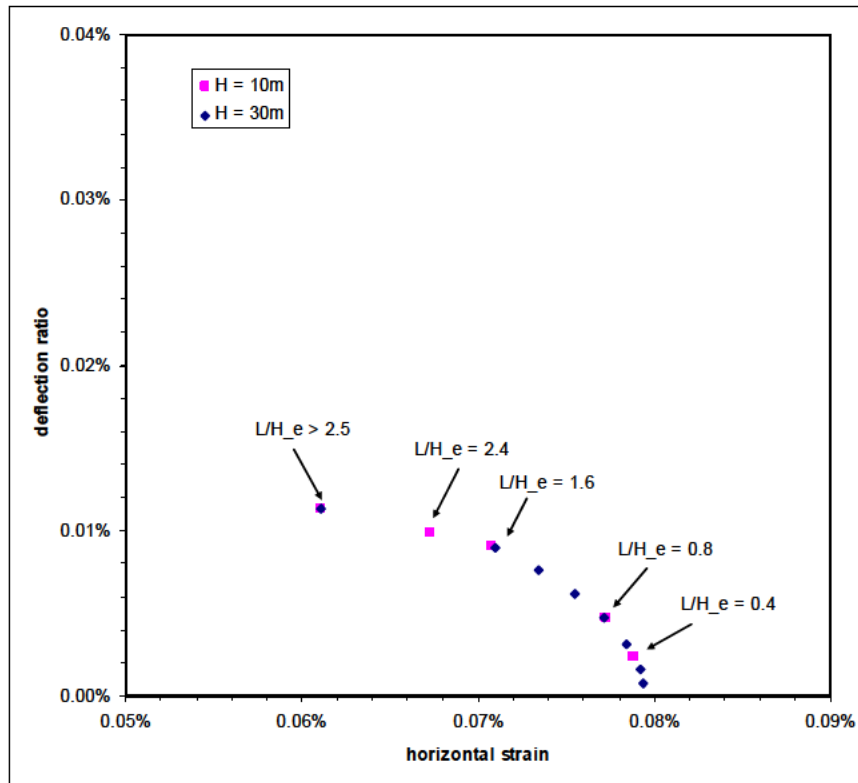
Crossrail: Settlement Estimation Procedure

Box Excavations and Shafts

Field data from New & Bowers (1994) compared with proposed estimation of horizontal displacement

Figure

9



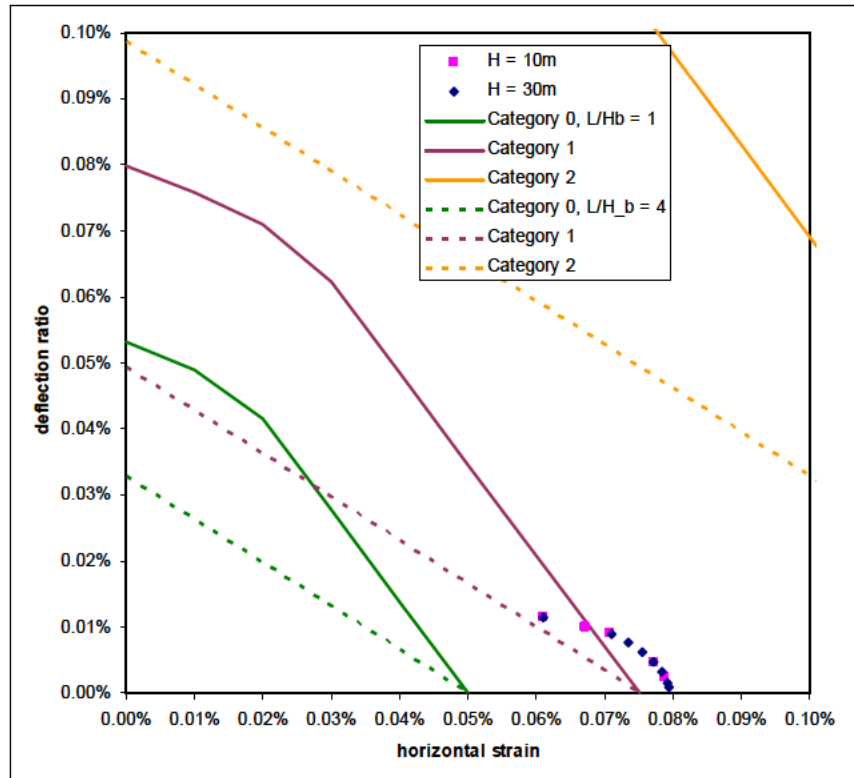
Crossrail: Settlement Estimation Procedure

Box Excavations and Shafts

Building distortion parameters due to box excavation for different geometries

Figure

10



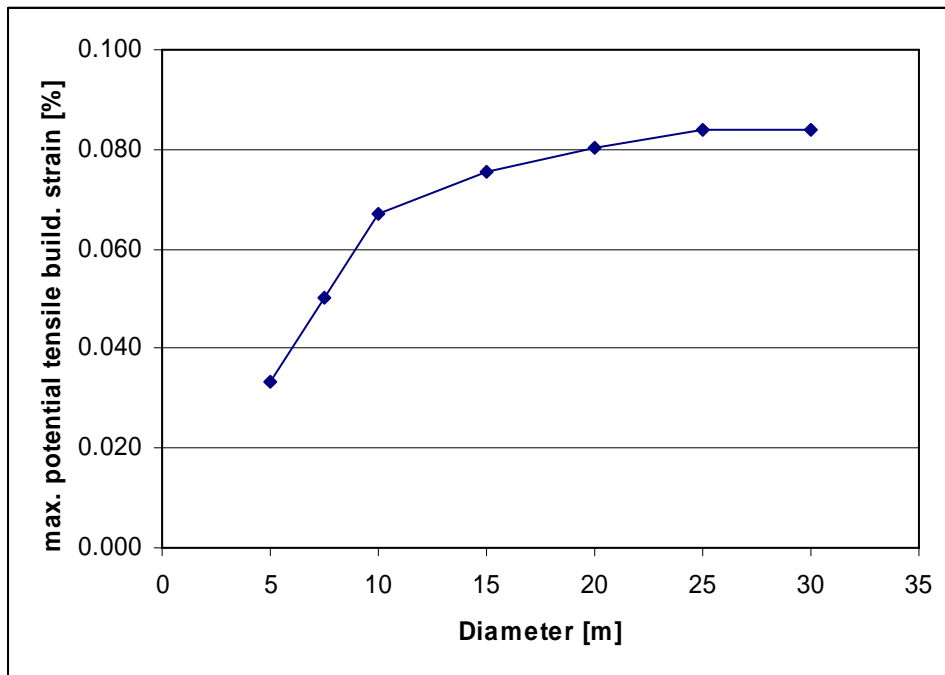
Crossrail: Settlement Estimation Procedure

Box Excavations and Shafts

Building distortion due to box excavation for different geometries compared with damage categories

Figure

11



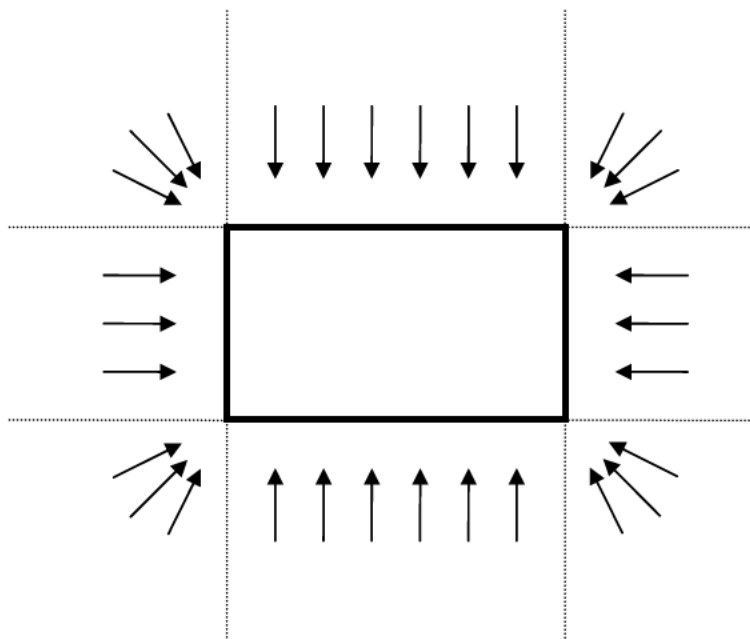
Crossrail: Settlement Estimation Procedure

Box Excavations and Shafts

Relationship between maximum value of potential building strain with shaft diameter

Figure

12



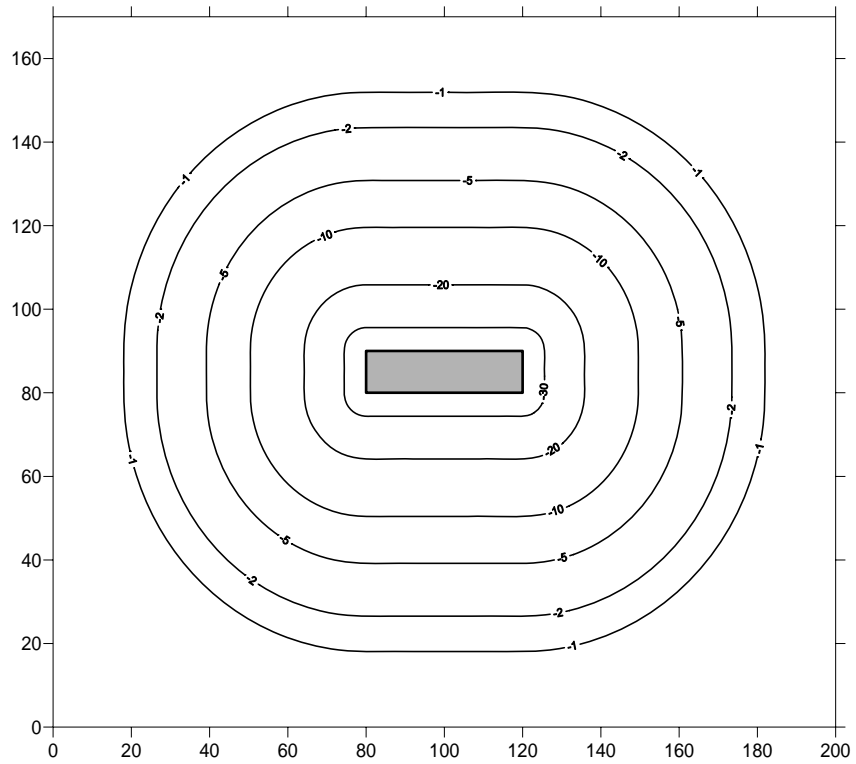
Crossrail: Settlement Estimation Procedure

Box Excavations and Shafts

Direction of horizontal soil movement around rectangular box

Figure

13



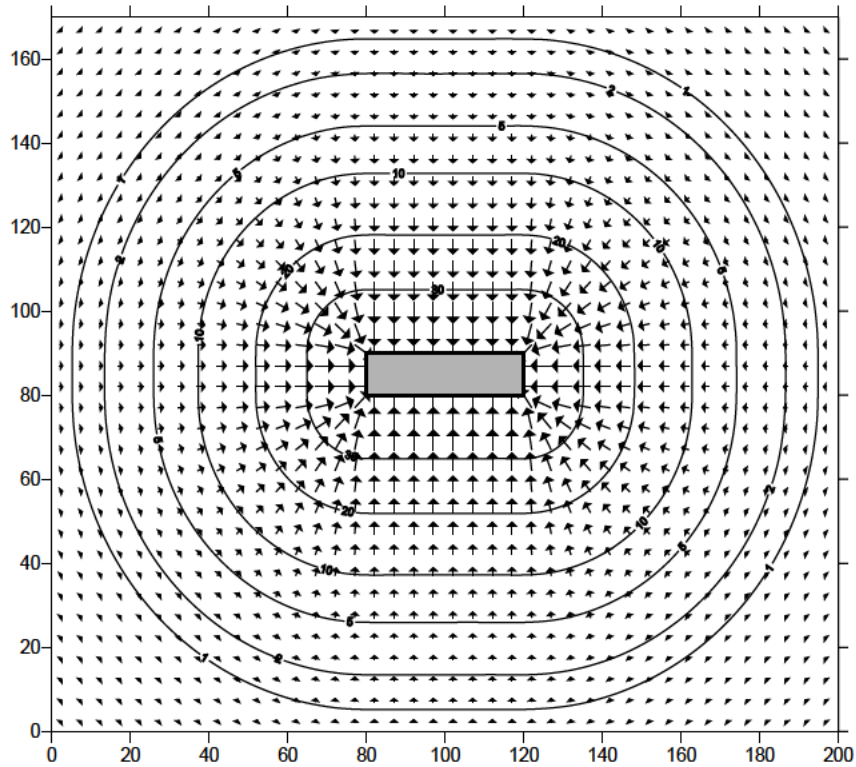
Crossrail: Settlement Estimation Procedure

Box Excavations and Shafts

Contours of surface settlement around rectangular box ($H_e = 20m$)

Figure

14



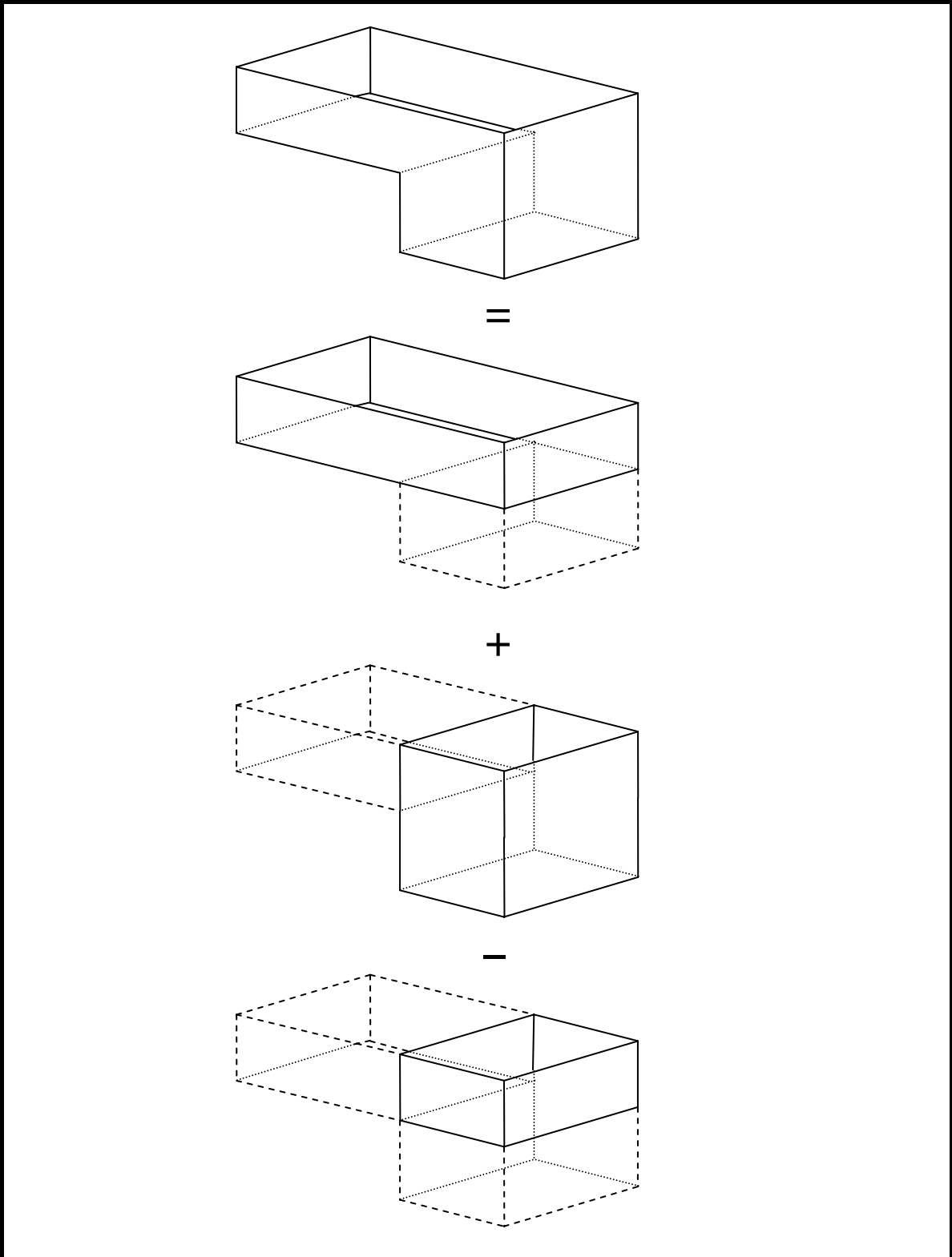
Crossrail: Settlement Estimation Procedure


Box Excavations and Shafts

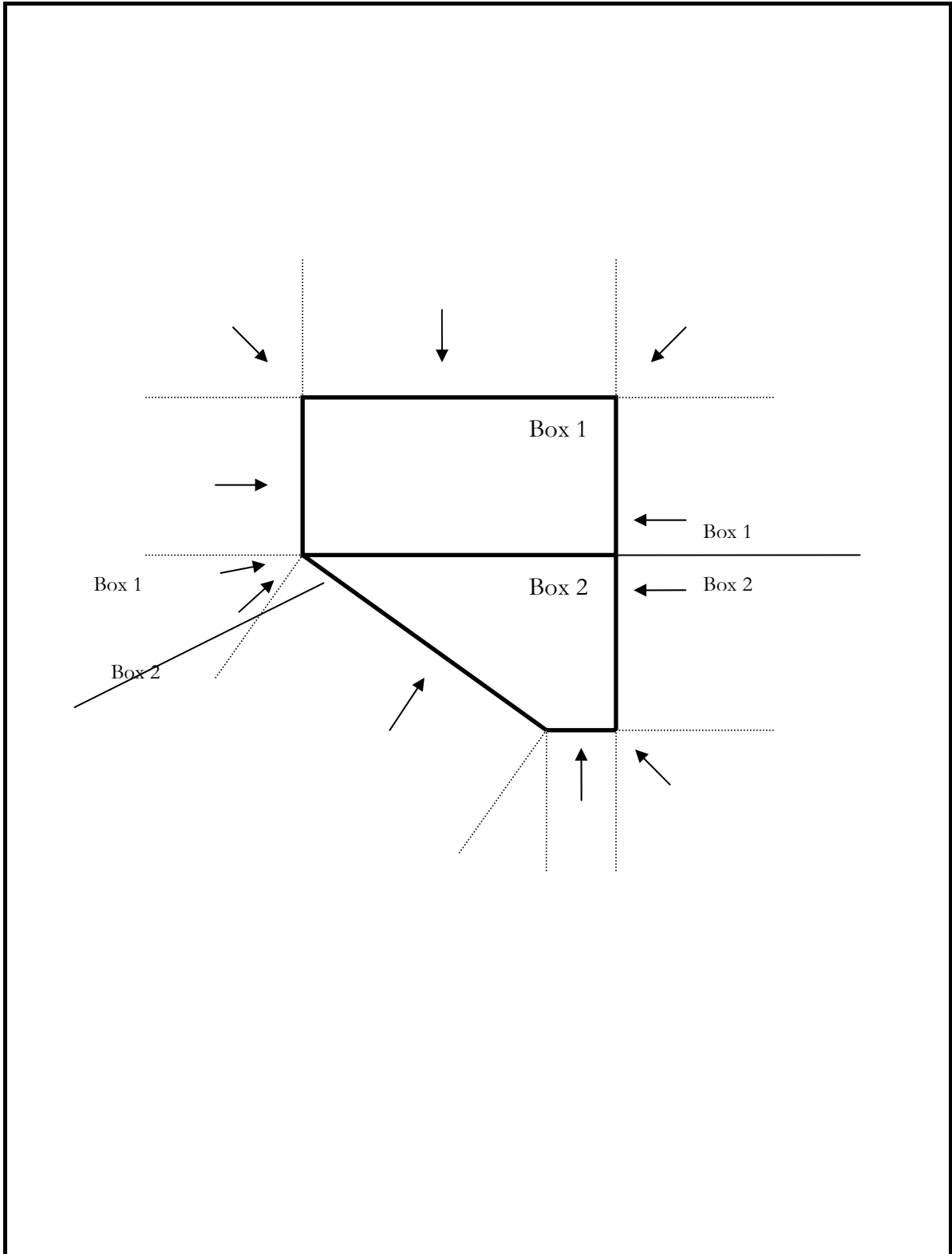
Contours & vectors of horizontal surface movement around rectangular box ($H_e = 20\text{m}$)


Figure

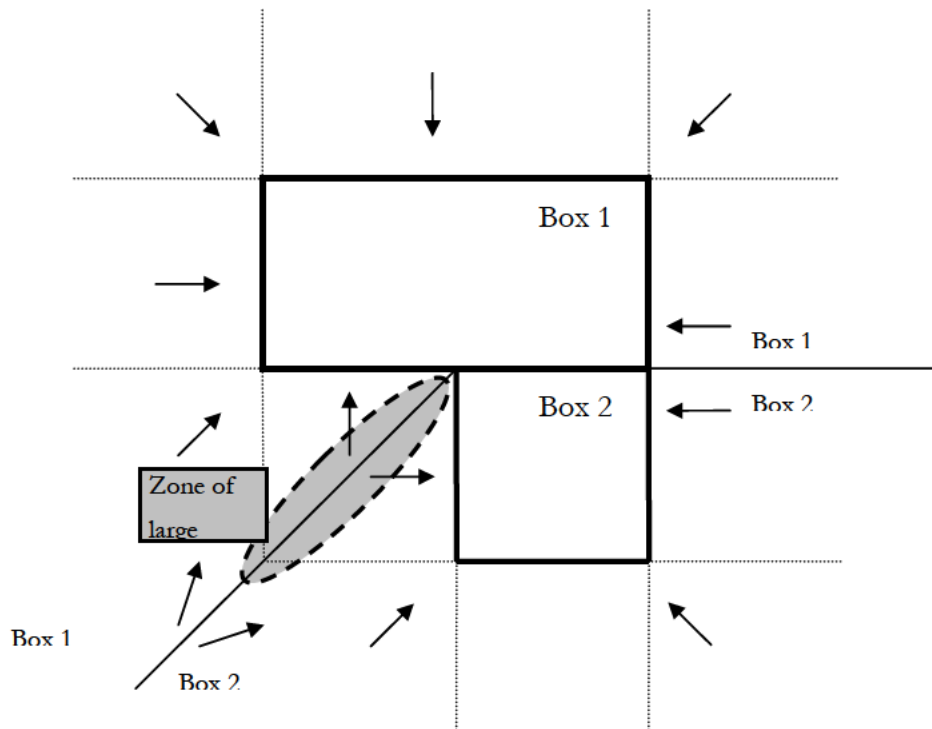
15



	Crossrail: Settlement Estimation Procedure Box Excavations and Shafts	Figure 16
	Combination of boxes to model irregular box shapes	



	Crossrail: Settlement Estimation Procedure Box Excavations and Shafts	Figure 17
	Settlement behaviour around irregular shaped box	



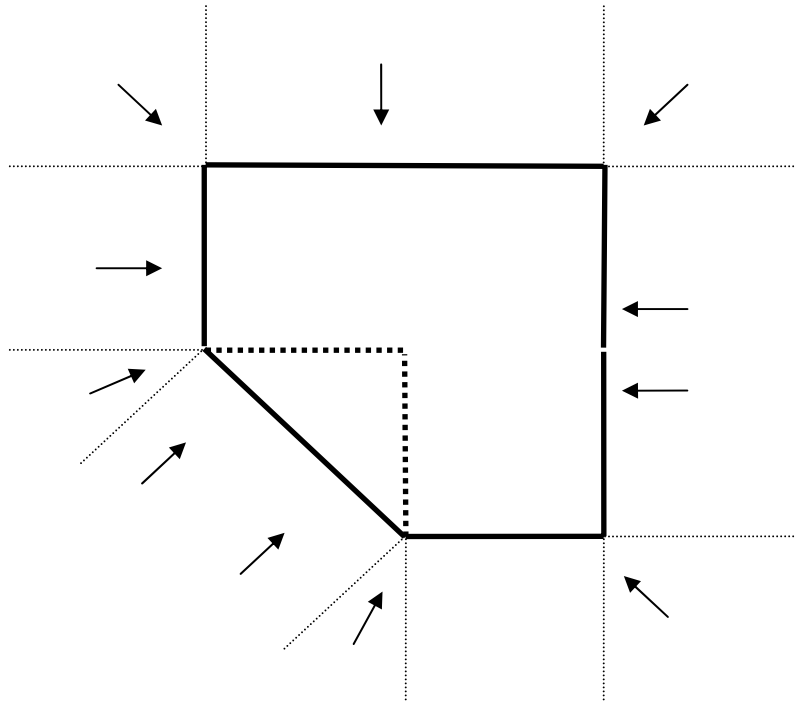
Crossrail: Settlement Estimation Procedure

Box Excavations and Shafts

Settlement behaviour in vicinity to a convex corner

Figure

19



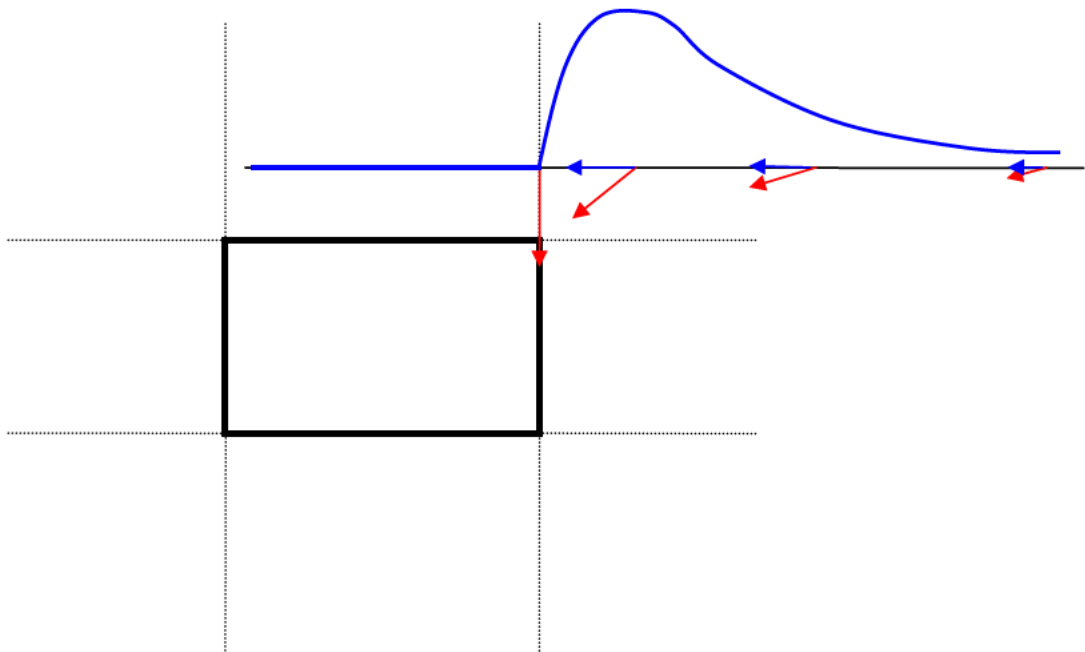
Crossrail: Settlement Estimation Procedure

Box Excavations and Shafts

Simplification of convex box to concave box

Figure

20



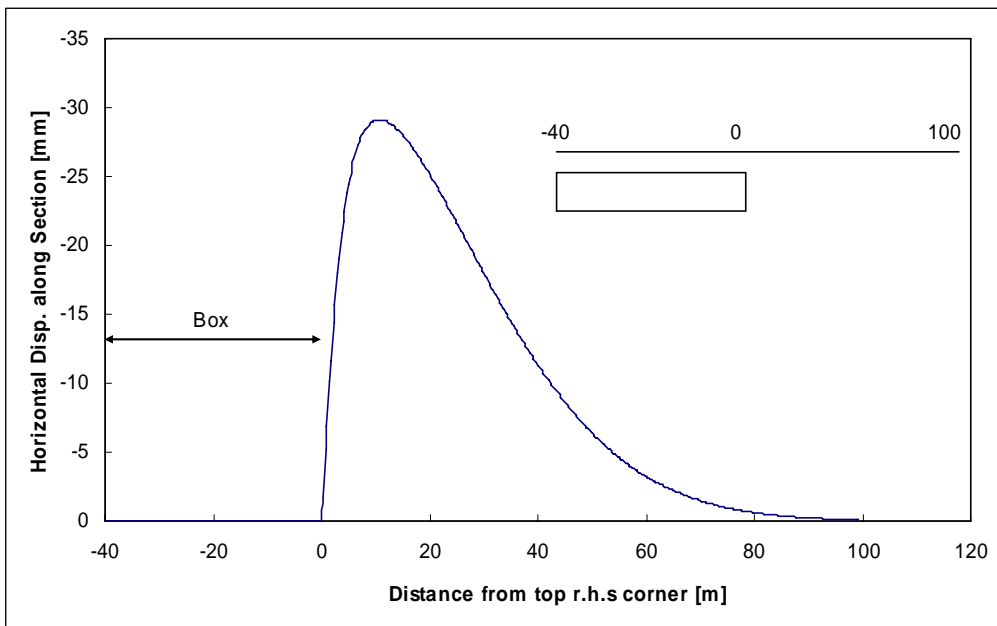
Crossrail: Settlement Estimation Procedure

Box Excavations and Shafts

Horizontal soil movement along a section in the vicinity of a corner

Figure

21



Crossrail: Settlement Estimation Procedure

Box Excavations and Shafts

Horizontal soil movement along a section in the vicinity of a corner
(result from calculation)

Figure

22

Figure Captions (needed for JNF cross-referencing)

Figure 1: Normalised settlement of case studies, (including data from CIRIA (2002))

Figure 2: Geometry of boxes and shafts from case studies compared with Crossrail cases.

Figure 3: Settlement of case studies (deep basement excavations only).

Figure 4: Proposed settlement behaviour due to box excavation

Figure 5: Horizontal soil movement of case studies from literature review (after CIRIA, 2002)

Figure 6: Geometry of horizontal ground movement

Figure 7: Settlement parameters for shafts.

Figure 8: Field data from New & Bowers (1994) compared with proposed settlement estimation.

Figure 9: Field data from New & Bowers (1994) compared with proposed estimation of horizontal displacement.

Figure 10: Building distortion parameters due to box excavation for different geometries.

Figure 11: Building distortion due to box excavation for different geometries compared with damage categories.

Figure 12: Relationship between maximum value of potential building strain with shaft diameter.

Figure 13: Direction of horizontal soil movement around rectangular box.

Figure 14: Contours of surface settlement around rectangular box ($H_c = 20\text{m}$)

Figure 15: Contours & vectors of horizontal surface movement around rectangular box ($H_c = 20\text{m}$)

Figure 16: Combination of boxes to model irregular box shapes.

Figure 17: Settlement behaviour around irregular shaped box.

Figure 18: Settlement contours around irregular shaped box (black); contours if the two sub-boxes are treated independently (orange, dotted).

Figure 19: Settlement behaviour in vicinity to a convex corner

Figure 20: Simplification of concave box to convex box

Figure 21: Horizontal soil movement along a section in the vicinity of a corner

Figure 22: Horizontal soil movement along a section in the vicinity of a corner (result from calculation)